Metallurgy and materials
INOX 2010

Numerical and experimental assessment of stainless and carbon bolted tensioned members with staggered bolts

Avaliação numérica e experimental de membros tracionados em aço carbono e aço inoxidável com parafusos defasados

João de Jesus dos Santos
PGECIV - Post Graduate Program in Civil Engineering, UERJ, Brazil
paraduc@yahoo.com.br

André Tenchini da Silva
PGECIV - Post Graduate Program in Civil Engineering, UERJ, Brazil
andretsilva@gmail.com

Luciano Rodrigues Ornelas de Lima
Structural Engineering Department, UERJ, Brazil
luciano@eng.uerj.br

Pedro Colmar Gonçalves da Silva Vellasco
Structural Engineering Department, UERJ, Brazil
vellasco@eng.uerj.br

Sebastião Arhur Lopes de Andrade
Structural Engineering Department, UERJ, Brazil
andrade@civ.puc-rio.br

José Guilherme Santos da Silva
Structural Engineering Department, UERJ, Brazil
jgss@eng.uerj.br

Abstract

Current stainless steel design codes, like the Eurocode 3, part 1.4, (2006), are still largely based on analogies with carbon steel structural behavior. The net section rupture represents one of the ultimate limit states usually verified for structural elements submitted to normal tension stress. An investigation aiming to evaluate the tension capacity of carbon and stainless steel bolted structural elements was performed and in this article, the results are discussed and compared in terms of stress distribution, and force-displacement curves, among others. The result assessment was done by comparisons to the Eurocode 3 (2003) provisions for carbon and stainless steels. The investigation indicated that when stainless steel is used in certain structural engineering applications like joints under tension forces, the current design criteria based on deformation limits need to be re-evaluated, especially due to the differences in the yields for ultimate deformation and stress ratios.

Keywords: Stainless steel, tension resistance, nonlinear analysis, bolted joints, finite element method.

Resumo

As normas atuais de projeto de estruturas em aço inoxidável, como o Eurocódigo 3, parte 1.4 (2006), são, em grande parte, baseadas em analogias assumidas com o comportamento de estruturas desenvolvidas com aço carbono. A ruptura da seção transversal representa um dos estados-limites últimos usualmente verificados para elementos estruturais submetidos a tensões normais de tração. Esse artigo apresenta uma investigação para se avaliar a resistência à tração de elementos aparafusados em aço carbono e aço inoxidável. Os resultados são discutidos e comparados em termos de distribuição de tensões, curvas carga-deslocamento, entre outros. Esses resultados foram comparados com as recomendações de projeto do Eurocódigo 3, para aço carbono e aço inoxidável, respectivamente. Essa investigação indicou que, quando o aço inoxidável é utilizado em certas aplicações da engenharia estrutural, como ligações submetidas a esforços de tração, o critério atual de dimensionamento, baseado em deformações-limites precisa de ser reavaliado, especialmente devido às diferenças elevadas de tensões de escoamento e de ruptura, respectivamente.

Palavras-chave: *Aço inoxidável, resistência à tração, análise não-linear, ligações aparafusadas, método dos elementos finitos.*

1. Introduction

Stainless steel has been used in various types of constructions, due to its main characteristics associated with high corrosion resistance, durability, fire resistance, ease of maintenance, appearance and aesthetics (Gardner and Nethercot, 2004). Stainless steel is indicated, as a structural element in construction for multiple reasons. Its high ductility allows its use in structures subjected to cyclic loadings, enabling the dissipation of the energy before structural collapse. Despite these facts, current stainless steel design codes like the Eurocode 3, part 1.4, (2003), are still largely based on carbon steel structural analogies.

The search for a broader understanding of the actual behavior of stainless steel joints has motivated investigations in various research centers like: Burgan et al. (2000), Gardner and Nethercot (2004) and Bouchair et al (2008). The motivation was the search for the most cost-effective structure resulting from an optimum joint design, as well as an improvement of the joint fabrication and assembly costs. Experimental studies indicated that different types of collapses, especially due to serviceability limitations, were observed in stainless steel joints with thin and thick plates under shear. This article presents an investigation aiming to evaluate the tension capacity of carbon and stainless steel bolted structural elements. The results are discussed and compared in terms of the stress distribution, and force-displacement curves, among others. Assessment of the results was done by comparisons to the Eurocode 3 (2003) provisions for carbon and stainless steels.

2. Eurocode 3 design code provisions

The current investigation uses the European code for stainless steel elements - Eurocode 3, pt 1.4 (2003). In this design standard, the failure modes for a plate with staggered holes under tension axial forces are governed by two ultimate limit states: the gross area yield and the net area tension rupture. The presence of staggered holes in the transversal section (see Figure 1), makes it difficult to immediately identify the plate's critical net section. This problem is not new, since Cochrane (1922), performed one of the first attempts to characterize staggered bolted connection failure modes by using Equation (1) below. This expression adds a term to the original net width to obtain the final net section area and it is present in major steel design codes all over the world.

$$b_n = b - d_b + \frac{s^2}{4p} \tag{1}$$

In the above equation, b is the plate width, d_b is the bolt diameter, s and p represent the staggered center to center hole distances measured parallel and perpendicular to the member axis

Eurocode 3, part 1.4, (2003) establishes the guidelines for the stainless steel plate design submitted to axial tension forces. As cited before, the structural failure is associated to the smallest axial tension force obtained considering two limiting states: gross cross-section plastic resistance given by Equation (2), or the ultimate net cross-section tension rupture expressed by Equation (3).

$$N_{pl,Rd} = \frac{A_g \cdot f_y}{\gamma_{M0}} \tag{2}$$

where $N_{pl,Rd}$ is the tension design plastic resistance, A_g is the plate's gross area, f_y is the steel's yielding stress, γ_{M0} is the partial safety factor, in this case equal to 1.

$$N_{u,Rd} = \frac{k_r \cdot A_n \cdot f_u}{\gamma_{M2}} \quad \text{with} \quad k_r = (1 + 3r(d_0/u - 0.3)) \tag{3}$$

where A_n is the net cross-section plate area, f_u is the steel tension rupture stress, k_r is a factor for stainless steel material, γ_{M2} is the partial safety factor, equal to 1.25, r is the ratio between the number of bolts at the cross-section and the total joint bolt number, d_0 is the hole diameter, $u = 2.e_2$ but $u \leq p_2$ where e_2 is the edge distance measured from the bolt hole center to its adjacent edge, in the direction perpendicular to the load direction and p_2 is the hole center-to-center distance, perpendicular to the load axis.

The tension plate design has also some additional provisions: in bolted joints, the hole width should be considered 2 mm larger than the nominal bolt diameter, perpendicular to the applied force direction; in the case of staggered holes, when a diagonal direction to the load axis or zigzag is considered, the net width should be calculated first deducing from the initial gross width, all the holes present in it, and after that adding for each staggered holes a value equal to $s^2/4p$, where s and g, correspond to the considered longitudinal and traversal hole spacing; the bolted joint critical net width is the smallest evaluated net width for all the possible net ruptures.

3. Experimental investigations

An innovative experimental program was used to evaluate the tension capacity of carbon and stainless steel plates with staggered bolts. The experiments involved bolted cover plate joints made of stainless steel A304 and carbon steel USI300 (Santos, 2008). All the geometrical properties for the tests are presented in Table 1. The bolted joints were made

of two, 3 mm thick, stainless and carbon steel plates and two, 15 mm thick, carbon steel plates used for load transfer to the 3mm plate with a 5 mm gap - see Figure 2(A). The horizontal bolt pitch, *s*, was modified in each test and the vertical bolt pitch, *p*, was 55 mm (see Figure 1). The bolted cover plate joint tests were carried out on a 600kN Universal Lousenhausen test machine; see Figure 2(B). The strain measurements were performed using linear strain gauges located in both stainless steel plates named SG in Figure 1.

The tensile coupons test curves presented a nonlinear expected behavior, mainly for the stainless steel – see Figure 2(C). The stainless steel yield stress was determined using a straight line parallel to the initial stiffness at a 0.2% deformation, leading to a value equal to 350.6 MPa while the ultimate tension stress was 710.7 MPa. For the carbon steel, these values were equal to 386.8 MPa and 478.7 MPa, respectively. Figure 2(C) also presents the results of a well-known true stress versus true strain curve used in the finite element modeling, due to the large strain and stresses associated with the investigated problem.

Figure 3 presents the comparison

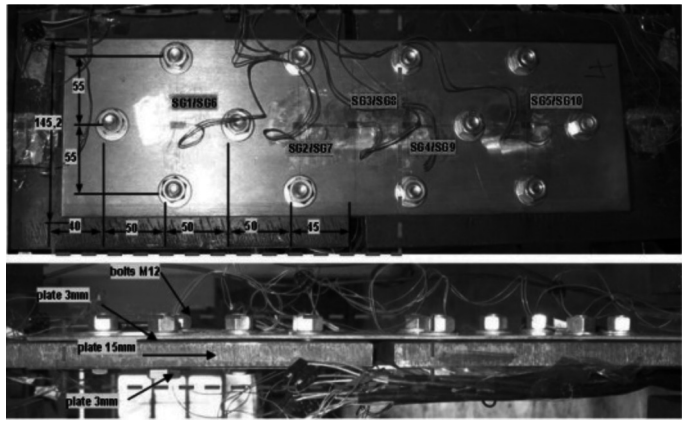

Figure 1
Cover plate joint detail and strain gauges location.

ID	s (mm)	p (mm)	e_1 (mm)	e_2 (mm)	d_0 (mm)	STEEL	t_{base} (mm)	bolts
E3_CARB_S50	50	55	40	17.6	14.7	carbon	15	6
E4_CARB_S30	30	55	40	17.6	14.7	carbon	15	6
E5_STAIN_S50	50	55	40	17.6	14.7	stainless	15	6
E6_CARB_S30_P10	30	55	40	17.6	14.7	carbon	10	6
E7_STAIN_S30	30	55	40	17.6	14.7	stainless	15	6
E8_CARB_S50_P8	50	55	40	17.6	14.7	carbon	8	6
E9_STAIN_S23	23	55	40	17.6	14.7	stainless	15	6

Table 1
Summary of experimental tests (Santos, 2008).

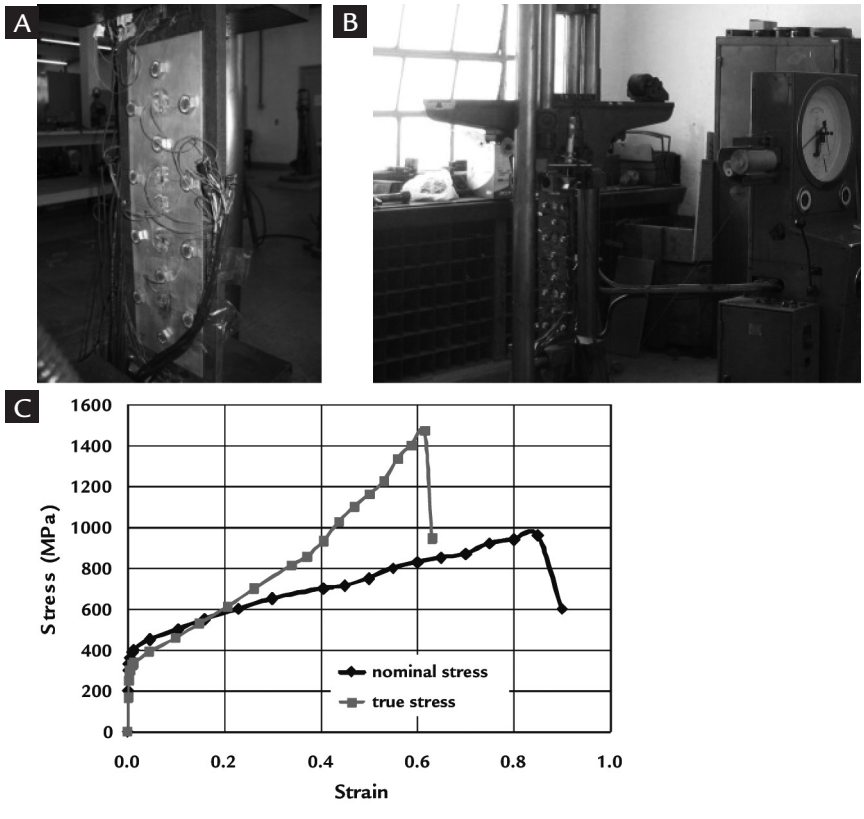

Figure 2
Santos et al. (2008) test layout.
A) cover plate joint detail.
B) Universal test machine, 600kN.
C) Stress versus strain curves for the stainless steel A304.

between the results from tests E3_CARB_S50 and E5_STAIN_S50 in terms of the load *versus* axial displacement curves. This figure depicts the experimental ultimate loads of 310.0 kN and 469.4 kN for E3_CARB_S50 and E5_STAIN_S50 tests, respectively. According to the Eurocode 3, (2003), Equations (2) and (3), for the E3_CARB_S50 test, the design resistances were 337.0 kN for gross cross-section plastic resistance and 298.7 kN for ultimate net cross-section tension rupture (section with three holes). While for the E5_STAIN_S50 test, these values were 305.5 kN and 810.8 kN (net section with three holes), respectively. The partial safety factor was taken to be equal to 1.0. Figure 3 also indicates that in both tests, the test rupture occurred in the section represented by two holes near the joint symmetry axis. For the carbon steel test E3_CARB_S50, the theoretical and experimental values presented a good agreement but the stainless steel test E5_STAIN_S50 presented a larger difference in terms of the ultimate design equation and test loads. Figure 3 also presents the results for tests: E4_CARB_S30 and E7_STAIN_S30. The ultimate loads were 303.6 kN and 545.8 kN for E4_CARB_S30 and E7_STAIN_S30 tests. According to the Eurocode 3 (2003), Equations. (2) and (3), for the E4_CARB_S30 test, the design resistances were 337.0 kN for gross cross-section plastic resistance and 291.7 kN for ultimate net cross-section tension rupture (section with three holes). For the E5_STAIN_S50 test, these values were 305.5 kN and 791.9 kN (net section with three holes), respectively. Figure 4 indicates that in both tests, the rupture occurred in the section with the two holes nearest to the joint symmetry axis. Again the carbon steel test E3_CARB_S50 theoretical and experimental values presented a good agreement while the stainless steel test E5_STAIN_S50, still showed a non-negligible difference for the ultimate design equation and test loads.

Considering the difference between the failure modes for the two stainless steel joints presented before, another test, E9_STAIN_S23, was done to investigate this issue where the horizontal bolt pitch was taken to be equal to 23mm. This value considered the increase in the difference between the load failure in sections with two and three bolts, respectively. According to Eurocode 3 (2003), for this test, the design resistances were 305.4 kN for gross cross-section plastic resistance and 787.7 kN for ultimate net cross-section tension rupture (section with three holes). Figure 4(a) presents the load *versus* displacement for this test where the ultimate load was equal to 526.5 kN. It can also be observed that the joint rupture occurred in the net section passing through three bolts, in agreement with the Eurocode 3 (2003). Despite this fact, the design equation and the tests collapse loads still had some difference. A summary of these results is presented in Table 2. It may be concluded that for carbon steel joints, a good agreement was observed comparing the theoretical and experimental results. Alternatively, for the stainless steel joints, larger differences were found in terms of ultimate (rupture) loads.

Another key issue undertaken involved the assessment of the influence of the load application plate thickness, adopted initially equal to 15mm (E3_CARB_S50 and E4_CARB_S30). Two

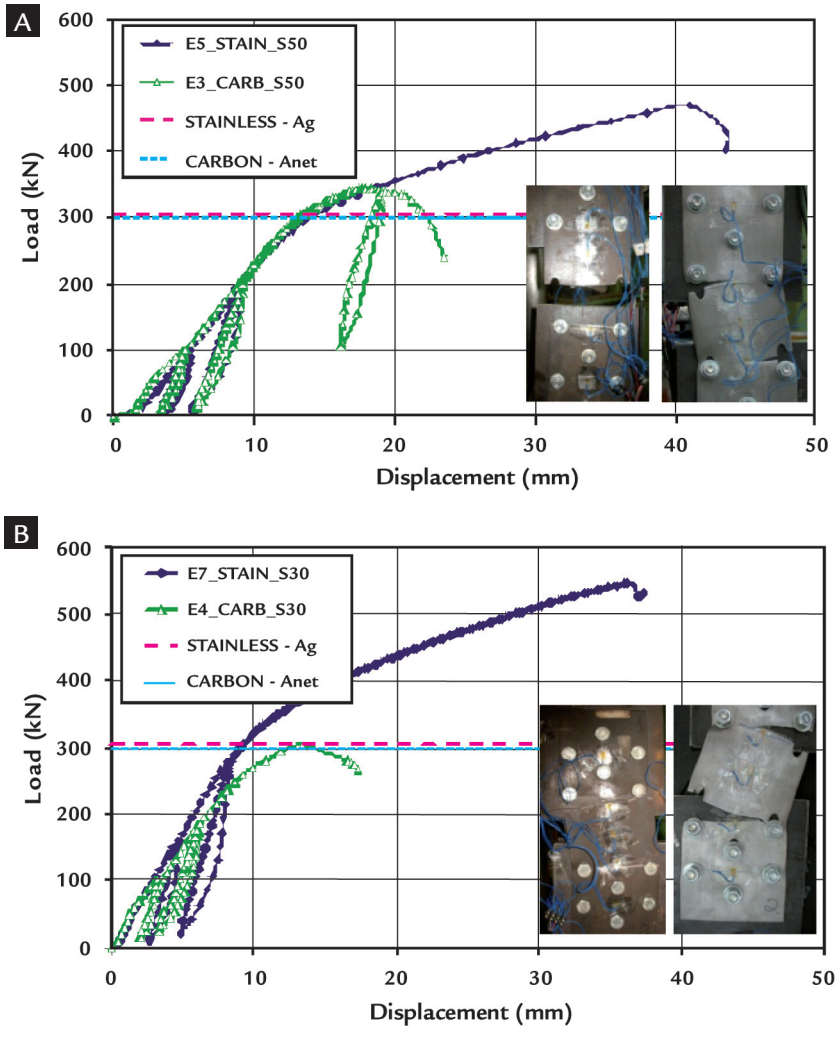

Figure 3
Load versus displacement curves – part I (Santos, 2008).
A) E3_CARBON_S50 & E5_STAIN_S50
B) E4_CARBON_S30 & E7_STAIN_S30.

other tests were performed, E6_CARB_S30_P10 (load plate thickness equal to 10 mm) and E8_CARB_S50_P8 (load plate thickness equal to 8 mm). Comparing the E3, E8 and E4 tests with E6, Figure 4(b), it may be concluded that the load application plate thickness significantly alters the joint response in terms of ultimate load and associated failure mode.

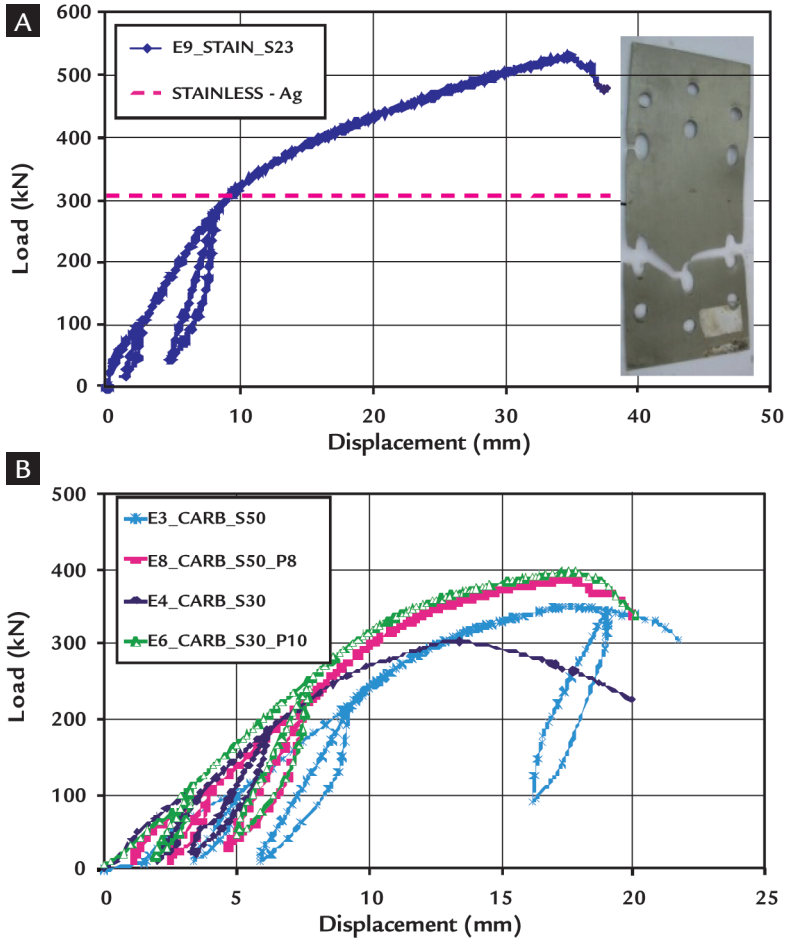

Figure 4
Load *versus* displacement curves – part II(Santos, 2008).
A) E9_STAIN_S23.
B) Load plate thickness variation.

ID	Experimental Failure Mode	Experimental Ultimate Load (kN)	EC3 Failure Mode	EC3 Ultimate Load (kN)	% EXP / EC3
E3_CARB_S50	2H	310.0	3H	298.3	3.9
E4_CARB_S30	2H	296.0	3H	282.5	4.8
E5_INOX_S50	2H	480.0	AB	302.9	58.5
E6_CARB_S30_P10	3H	309.5	3H	282.5	9.6
E7_INOX_S30	2H	459.0	AB	302.9	51.5
E8_CARB_S50_P8	2H	326.0	2H	282.5	13.3
E9_INOX_S23	3H	436.0	AB	302.9	43.9

Table 2
Summary of experimental tests (Santos, 2008).
2H: Two hole net rupture.
3H: Three hole net rupture.
AB: Gross section yielding.

4. Numerical investigation

Finite element numerical analyses provide a relatively inexpensive and time efficient alternative to physical experiments. Despite this fact, due to their nature, these numerical simulations have to be properly calibrated against experimental test results (Silva, 2009). If the validity of FE analysis is assured, it is possible to investigate the structural behavior against a wide range of parameters with the FE model. A finite element model was used to investigate the tension capacity of cover plate joints developed with the aid of the Ansys 11 (2008) FE package. The numerical model adopted solid elements (SOLID45) defined by eight nodes with three degrees of freedom per node: translations in the nodal x, y and z directions.

Contact elements (CONTA174 and TARGE170) presented in the Ansys 11 (2008) Elements Library, were considered between the plates and between the holes and the bolt shanks. The load was applied by means of axial displacements in the load plate such as presented in Figure 5. In this figure, it is also possible to observe that the bolt head and nuts were simulated through UZ displacements restraints at the hole's adjacent area. Figure 5 presents a typical mesh configuration of the complete model. It is emphasized here that only half of the model was considered using symmetry conditions sufficient to characterize the joint ultimate limiting states.

The adopted material properties were: Young's modulus of 210 GPa (see

Figure 2) and a Poisson's coefficient of 0.3. As previously mentioned, stainless steel true stress *versus* true strain curves with a nonlinear behavior were adopted using data from the tensile coupons tests - Figure 2(C). A full nonlinear analysis was performed for the developed numerical model. The material non-linearity was considered using a *von Mises* yield criterion associated to a multi-linear stress-strain relationship and isotropic hardening response. The geometrical non-linearity was introduced in the model by using an Updated Lagrangean formulation. This procedure represents the full structural assessment of the analyzed bolted joints, and may be summarized in several outputs, namely the stress distribution (that detects, among other data, first yield), or the force versus displacement curve for any node within the connection.

Figure 6 presents the load versus displacements curves for each individual test, where it can be observed that the ultimate load of experiments E5_INOX_S50, E7_INOX_S30 e E9_INOX_S23 were: 389 kN, 389 kN and 385 kN, respectively. All the numerical model loads were situated in an interval between the experimental loads and the Eurocode 3 part 1.4 (2003) estimated values.

In order to validate the proposed numerical model, a series of comparisons will be presented in terms of load versus strain curves for specific points that were measured in the experimental program. Figure 7 presents numerical and experimental strain comparisons for the E5_INOX_S50 specimen, measured in the region close to the joint center line. It can be observed that a similar response was found in the numerical and experimental curves, for strain gauges 2(4) and 3(8). However, the numerical model presented in the plastic range had a stiffness value lower than its experimental counterparts. Figure 8 depicts load vs. strain curves for the E7_INOX_S30 test, where it can be observed that the numerical results were not as good as the previous tests,

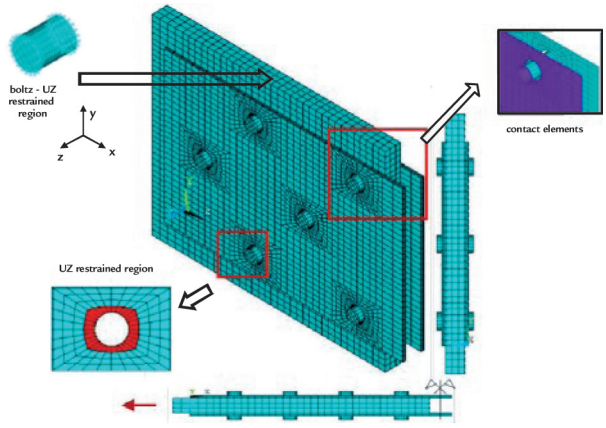

Figure 5
Finite element model and contact elements (Silva, 2009).

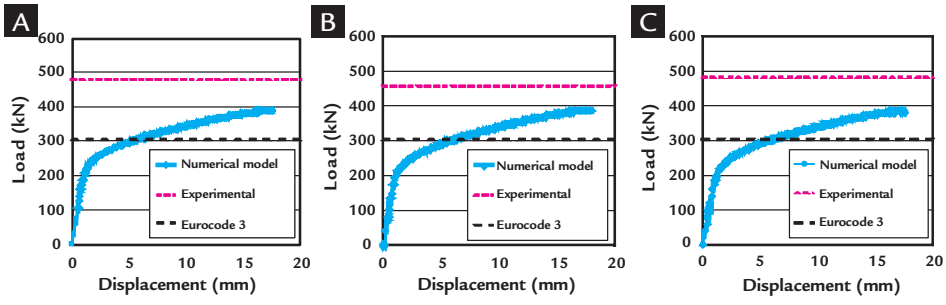

Figure 6
Stainless steel load *versus* displacement curves (Silva, 2009).
A) E5_INOX_S50 specimen.
B) E7_INOX_S30 specimen.
C) E9_INOX_S23 specimen.

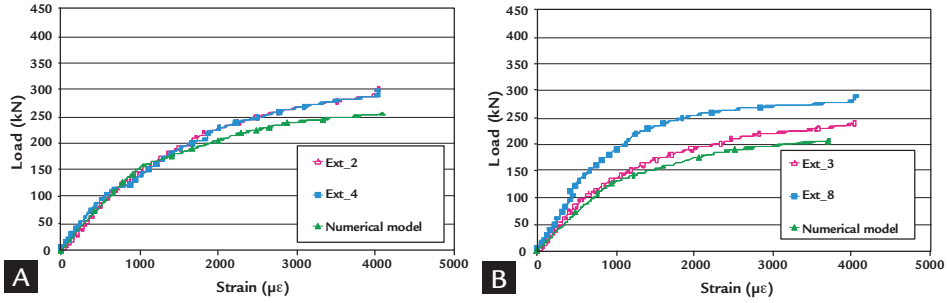

Figure 7
Load vs strain (experimental and numerical) - E5_INOX_50 (Silva, 2009).
A) Strain gauges 2 and 4.
B) Strain gauges 3 and 8.

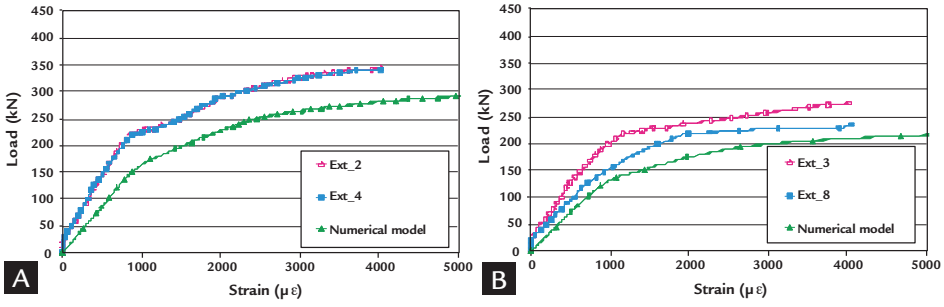

Figure 8
Load vs strain (experimental and numerical) - E7_INOX_30 (Silva, 2009).
A) Strain gauges 2 and 4.
B) Strain gauges 3 and 8.

presenting a lower stiffness and achieving larger strains than its experimental counterparts. Alternatively, the results of E9_INOX_S23 tests, Figure 9, indicated a good similarity between the numerical and test evidences.

The plate section at which the stainless steel net area rupture failure mode occurred was determined with the aid of Figure 10 where load vs. strain curves are illustrated for a point located at the plate cross section with two bolt holes at the horizontal symmetry axes. From this graph, it can be observed that as the horizontal distance between two bolt holes increases, the magnitude of the stresses on the bolt present in adjacent section diminishes. For example, for a 250kN load level, the left curve is associated to a strain level lower than the others, highlighting the net area rupture failure passing in a plate section with three bolt holes. On the other hand, for this load level, the E5_INOX_S50 numerical model highlights that the failure mode is associated to the net area rupture failure passing in a section with two bolt holes.

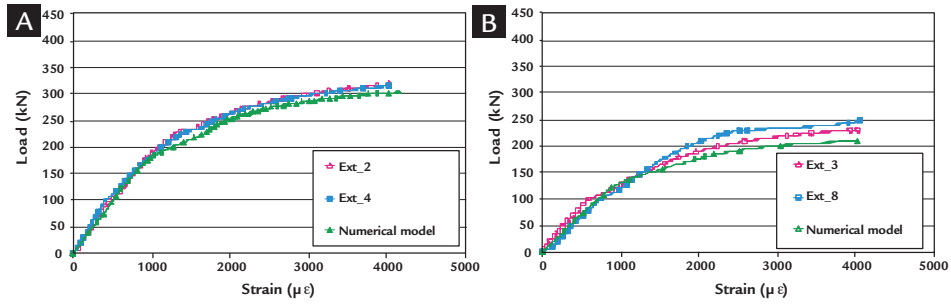

Figure 9
Load vs strain (experimental and numerical) - E9_INOX_23 (Silva, 2009).
A) Strain gauges 2 and 4
B) Strain gauges 3 and 8

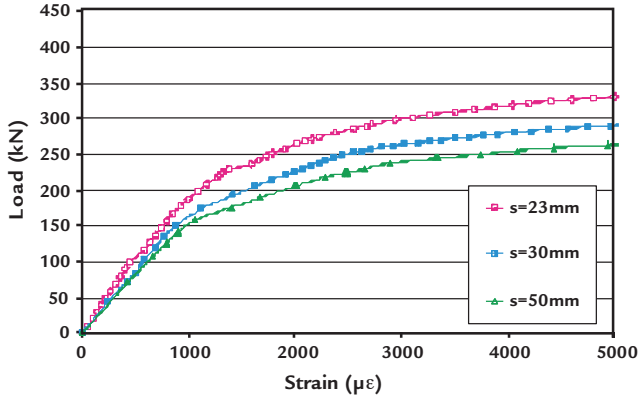

Figure 10
Load *versus* strain curves for all the numerical models (Silva, 2009).

5. Final considerations

This paper presented an experimental and numerical program to investigate the structural response of the carbon steel and stainless steel plates with staggered bolts under tension. Initially the experimental results were compared to theoretical results according to Eurocode 3, (2003), provisions. For carbon steel tests, a good agreement was reached between the design equation and the experiments; a fact that was not corroborated in the stainless steel tests, where large difference were observed, mainly in terms of the ultimate load. A possible explanation for these discrepancies could be related to the fact that the great majority of stainless steel structural design codes are still based on carbon steel analogies. At this point, it is interesting to observe that the stainless steel codes need to be improved in order to correctly evaluate the stainless steel structural element behavior. A finite element numerical model was also developed with the aid of the Ansys 11 (2008) and considered material and geometrical nonlinearities through the *von Mises* yield criterion and the Updated Lagrangian Formulation, respectively. The numerical model calibration was made against Santos (2008) experiments where the optimum mesh and element sizes were determined, Silva (2009).

Table 3 presents a comparison between the numerical results and the Eurocode 3 provisions (2003), for the already mentioned stainless steel tests (Santos, 2008). Differences of about 28% were found when the Eurocode 3 (2003) and the numerical models were compared. The numerical ultimate loads were less than their experimental counterparts for all the investigated specimens. This can be explained by the fact that the developed numerical models represent the joints in an idealized form, without imperfections or residual stresses. Another reason for these differences can be attributed to the fact that the stainless steel stress *versus* strain curve adopted in the finite element model was obtained through coupons specimens that are influenced by the rolling direction. The problem related to the numerical and experimental assessment of stainless and carbon bolted tensioned members is certainly much more complicated and it is influenced by several other design parameters. Further research in this area is currently being carried out, in order to consider imperfections, residual stresses and the coupons rolling directions.

On the other hand, differences varying from entre 12% up to 19% were found when the numerical and the experimental values were compared. These differences were also partly due to the natural conservatism present in most of the design standard Eurocode 3, part 1.4, (2003). This conservatism is largely due to the lack of experimental evidence regarding stainless steel response not yet present in literature. The investigation indicated that when stainless steel is used in certain structural engineering applications like joints under shear forces, the current design criteria based on deformation limits need to be re-evaluated, especially due to the differences in the yields for ultimate deformation and stress ratios.

Experimental tests	Experimental failure mode	Experimental ultimate load (kN)	Numerical failure mode	Numerical ultimate load (kN)	Difference Numerical x Experimental (%)	Difference Numerical x EC3 (%)
E5-INOX-S50	2H	480.0	2H	389	19.0	28.8
E7-INOX-S30	2H	459.0	2H / 3H	389	15.2	28.8
E9-INOX-S23	3H	436.0	3H	385	11.6	27.5

Table 3
Summary of experimental tests (Silva, 2009).

6. Acknowledgments

The authors gratefully acknowledge the Brazilian National and State Science Support Agencies: CAPES, CNPq and FAPERJ for the financial support granted to this research program. Thanks are also due to ACESITA and USIMINAS for donating the stainless and carbon steel plates used in the experiments.

7. Bibliographic references

ANSYS, Inc. Theory Reference, 2008. (version 11.0)

BOUCHAIR, J., AVERSENG, A., ABIDELAH. Analysis of the behaviour of stainless steel bolted connections. ***Internal Report - LaMI***, Blaise Pascal University, France, 2008

BURGAN B. A., BADDOO, N. R., GILSENAN, K. A. Structural design of stainless steel members - comparison between Eurocode 3, Part 1.4 and test results. ***Journal of Constructional Steel Research***, v. 54, n. 1, p.51-73, 2000.

COCHRANE, V. H. Rules for rivet hole deduction in tension members. ***Engineering News-Record***, v. 80, 1922.

EUROCODE 3, ENV 1993-1-1, 2003: Design of steel structures - Structures – Part 1-1: General rules and rules for buildings. ***CEN, European Committee for Standardisation***, 2003.

EUROCODE 3, ENV 1993-1-4, 2003: Design of steel structures – Part 1.4: General rules – Supplementary rules for stainless steel, ***CEN, European Committee for Standardisation***, 2003.

GARDNER, L., NETHERCOT, D. A. Experiments on stainless steel hollow sections — Part 1: Material and cross-sectional behaviour. ***Journal of Constructional Steel Research***, v. 60, n.9, p. 1291–1318, 2004.

SANTOS, J. de J. DOS, Comportamento estrutural de elementos em aço inoxidável, ***MSc in Civil Engineering***, State University of Rio de Janeiro, UERJ, Rio de Janeiro, Brazil, 2008. (In portuguese).

SILVA, A. T. da, Modelagem numérica de elementos tracionados em aço inoxidável com parafusos defasados, ***MSc in Civil Engineering***, State University of Rio de Janeiro, UERJ, Rio de Janeiro, Brazil, 2009. (In portuguese).

Paper submitted to INOX 2010- 10th Brazilian Stainless Steel Conference, September 20-22, Rio de Janeiro, Brazil. Revised accepted December, 28, 2012.